

See discussions, stats, and author profiles for this publication at: <https://www.researchgate.net/publication/231231122>

Influence of Ligand Geometry on the Dimensionality of Sn(II) Benzenedicarboxylate Crystal Structures

ARTICLE in CRYSTAL GROWTH & DESIGN · JULY 2010

Impact Factor: 4.89 · DOI: 10.1021/cg1005874

CITATIONS

8

READS

46

4 AUTHORS, INCLUDING:



Xiqu Wang

University of Houston

133 PUBLICATIONS 2,331 CITATIONS

[SEE PROFILE](#)



Tatyana Makarenko

University of Houston

7 PUBLICATIONS 38 CITATIONS

[SEE PROFILE](#)

Influence of Ligand Geometry on the Dimensionality of Sn(II) Benzenedicarboxylate Crystal Structures

Xiqu Wang, Lumei Liu, Tatyana Makarenko, and Allan J. Jacobson*

Department of Chemistry, University of Houston, Houston, Texas 77204-5003

Received May 1, 2010; Revised Manuscript Received June 19, 2010

ABSTRACT: Four new divalent tin benzenedicarboxylates (bdc) have been synthesized by hydrothermal techniques, and their structures have been determined from single crystal X-ray data. A chiral complex layer is formed by Sn^{II} and 1,2-bdc. In Sn(1,2-bdc)-II (**2**), such layers are stacked in a AA pattern, leading to a chiral and polar structure with the space group symmetry C2, while in Sn(1,2-bdc)-I (**1**) the same layer is alternately stacked with the mirror-image layer, leading to a structure with the space group C2/c. The one-sided coordination of Sn^{II} combined with the 120° angle of the carboxylate groups in 1,3-bdc results in the tubular structure of Sn(1,3-bdc) (**3**). The tubes are connected by very weak intertube Sn—O bonds. The compound Sn₃O(1,4-bdc)₂ (**4**) has a 3D framework structure based on Sn₃O triangular secondary building units that are cross-linked by the 1,4-bdc ligands. Strong π–π interactions occur between the neighboring phenyl rings.

Introduction

Benzenedicarboxylic acids (bdc) are among the most common ligands used for the construction of metal organic frameworks (MOFs) based on oxide clusters and metal oxide organic frameworks (MOOFs) based on infinitely extended oxide units.^{1–5} Sometimes, to facilitate the formation of structures with low dimensionality or with large voids, the bdc linkers have been partially replaced by terminating ligands such as 2,2'-bipyridine or water molecules.^{6,7} A similar terminating role may also be played by the electron lone pairs of metal cations such as Sn²⁺, which tend to have an asymmetric “one-sided” coordination environment.^{8,9} Compared to the large number of known MOFs and MOOFs built with transition metal divalent cations, similar compounds with main group lone-pair cations have been less explored. Remarkable structural diversity has been observed, however, in some Pb(II)- and Sn(II)-carboxylate systems.^{10–17} Recently, we reported a series of divalent tin terephthalates based on an 8-fold interpenetrated open framework with the composition [Sn₂(1,4-bdc)₃]²⁻. The site preference of the charge balancing alkali cations in nonframework sites determines whether the interpenetration of the frameworks is chiral or nonchiral.¹⁸ Some of these phases decompose in water to form a new compound, Sn₃O(1,4-bdc)₂, with a 3-dimensional structure, which can also be obtained by direct hydrothermal synthesis. Changing the 1,4-H₂bdc linker to 1,3-H₂bdc or 1,2-H₂bdc in the syntheses led to crystals with a tubular or layered structures, respectively. Different stacking arrangements of the Sn(1,2-bdc) layered enantiomers result in two polymorphs. Here we report on the synthesis and characterization of Sn(1,2-bdc)-I, **1**; Sn(1,2-bdc)-II, **2**; Sn(1,3-bdc), **3**; and Sn₃O(1,4-bdc)₂, **4**.

Experimental Section

Materials and Methods. All reactants were reagent grade and used as purchased without further purification. Elemental analyses were performed by Galbraith Laboratories (Knoxville, TN). Thermal

gravimetric analysis (TGA) was carried out on a TA Instruments thermogravimetric analyzer. The samples were first heated to 50 °C with a heating rate of 5 °C/min, held at 50 °C for 30 min to eliminate any surface water, and subsequently heated with a heating rate of 3 °C/min in air to 800 °C. The IR spectra were recorded on a Galaxy Fourier transform infrared 5000 series spectrometer at room temperature in the range 4000–400 cm⁻¹ using the KBr pellet method. Powder X-ray diffraction analyses were performed on a Phillips X'pert Pro diffractometer. Single-crystal X-ray diffraction data were collected on a Siemens SMART platform diffractometer outfitted with a Bruker Apex II area detector and monochromatized Mo Kα radiation at room temperature. The crystal structures were solved and refined with the Apex II software package.¹⁹ Crystal data and structure refinement details are given in Table S1 of the Supporting Information.

Synthesis of Sn(1,2-bdc)-I (1**) and Sn(1,2-bdc)-II (**2**).** In a typical synthesis of compounds **1** and **2**, a solution was first made by dissolving LiOH·H₂O (420 mg) and 1,2-H₂bdc (830 mg) in H₂O (20 mL). Two milliliters of the solution was then mixed with 107 mg of SnSO₄. The mixture was subsequently sealed in a Teflon vessel (23 mL inner volume) in air and heated at 160 °C for 3 days. Colorless platy crystals of phase **1** were recovered from the final solution (pH = 3.0) in high yield (~60% based on Sn). The crystals were washed with distilled water, *N,N*-dimethylformamide, and methanol and then dried in air. Elem. Anal.: C, 33.33% (calc 33.96%); H, 1.35% (calc 1.42%); Sn, 42.86% (calc 41.99%). IR (KBr): 3441 w, 1608 w, 1583 m, 1570 s, 1556 s, 1488 w, 1442 w, 1397 m, 1369 s, 1296 w, 1160 w, 1139 m, 1085 m, 1039 w, 868 m, 833 w, 764 m, 701 s, 656 m, 565 w, 472 m, 413 w cm⁻¹.

Thin lamellar crystals of phase **2** with a characteristic necktie shape occurred as a minor phase (<3%, estimated from observations under a microscope) together with **1** and were characterized by single crystal structure determination only. Efforts to improve the yield of **2** by adjusting reagent ratios and reaction temperatures have not been successful.

Synthesis of Sn(1,3-bdc) (3**).** Compound **3** was synthesized by mixing LiOH·H₂O (82 mg), 1,3-H₂bdc (498 mg), SnSO₄ (165 mg), and H₂O (3 mL). The mixture was subsequently sealed in a Teflon vessel (23 mL inner volume) in air and heated at 160 °C for 3 days. Colorless needles of **3** with lengths up to 2 mm were obtained with a yield of ~50% based on Sn. The final pH was 2.3.

Elem. Anal.: C, 33.58% (calc 33.96%); H, 1.47% (calc 1.42%); Sn, 42.26% (calc 41.99%). IR (KBr): 3430 m, 1634 w, 1603 m, 1593 m, 1528 s, 1511 s, 1481 m, 1414 s, 1398 s, 1384 s, 1280 w, 1167 w, 1075 w, 942 w, 740 s, 716 m, 679 w, 654 m, 621 w, 593 w, 562 m, 475 w, 428 m, 406 m cm⁻¹.

Synthesis of Sn₃O(1,4-bdc)₂ (4**).** Compound **4** was synthesized by hydrothermal reactions of a mixture of saturated aqueous solutions

*Corresponding author. Telephone: 713-742-2785. Fax: 713-742-2785. E-mail: ajjacob@uh.edu

of SnSO_4 (3 mL) and $(\text{TMA})_2(1,4\text{-bdc})$ (3 mL) [TMA = tetramethylammonium]. The mixture was sealed in a Teflon vessel (23 mL inner volume) in air and heated at 180 °C for 24 h, and then it was cooled in air to room temperature. Colorless plates of **4** were recovered from the final solution ($\text{pH} = 3.1$) by vacuum filtering and washing with distilled water, N,N -dimethylformamide, and methanol. The yield is ~30% based on Sn. Elem. Anal.: C, 27.24% (calc 27.42%); H, 1.11% (calc 1.14%); Sn, 51.35% (calc 50.85%). IR (KBr): 3445 w, 1544 m, 1535 m, 1519 s, 1505 s, 1407 m, 1382 s, 1370 s, 1347 s, 1318 m, 1143 w, 1107 w, 1016 w, 847 m, 821 m, 738 s, 569 w, 534 s, 518 m, 504 m, 486 w cm^{-1} .

Results

The IR spectra all exhibit characteristic bands of the dicarboxylate groups between 1300 and 1650 cm^{-1} . The absence of any strong absorption bands at approximately 1700 cm^{-1} confirms the complete deprotonation of the carboxyl groups, consistent with the crystal structure models from X-ray diffraction data. For compound **1**, TGA data show a sharp weight loss in the region 220–350 °C followed by a tail between 350 and 450 °C. The total weight loss of 47.3% corresponds to decomposition of the compound to SnO_2 (calcd 46.7%). The residue at 600 °C was confirmed to be SnO_2 by X-ray powder diffraction. Compound **3** shows a single sharp weight loss of 46.1% between 390 and 420 °C, corresponding to decomposition to SnO_2 (calcd 46.7%), as confirmed by X-ray powder diffraction on the residue at 800 °C. Similarly, compound **4** decomposes to SnO_2 in the temperature range 415–440 °C (weight loss obsd 35.1%, calcd 35.4%).

Crystal Structures of $\text{Sn}(1,2\text{-bdc})\text{-I}$ (1**) and $\text{Sn}(1,2\text{-bdc})\text{-II}$ (**2**).** The two polymorphs of $\text{Sn}(1,2\text{-bdc})$ are based on similar complex layers. In structure **2**, which has a higher refinement accuracy, the divalent tin atom is bonded to three oxygen atoms from three different 1,2-bdc ligands to form a SnO_3 triangular pyramid with strong $\text{Sn}-\text{O}$ bonds (2.195(3)–2.250(4) Å). As shown in Figure 1a, the pyramid is complemented by two weak $\text{Sn}-\text{O}$ bonds (2.535(3)–2.796(4) Å) to form a SnO_5 distorted hemioctahedron. One of the carboxylate groups of the 1,2-bdc ligand is roughly coplanar with the phenyl ring while the other is close to perpendicular to the phenyl ring. The former carboxylate group bridges two SnO_5 hemioctahedra with two short $\text{Sn}-\text{O}$ bonds, while the latter carboxylate group chelates to a third Sn atom with one short and one long $\text{Sn}-\text{O}$ bond. Two 1,2-bdc ligands with their phenyl rings almost perpendicular to each other bridge two SnO_5 hemioctahedra to form a “butterfly” unit (Figure 1b). Each such unit is connected with four neighbors by the chelating $\text{Sn}-\text{O}$ bonds to form an infinite layer (Figure 1c). The layer is chiral with the electron lone pairs of the Sn ions, assumed to be on the opposite side to the strong $\text{Sn}-\text{O}$ bonds, all pointing roughly toward the same edge of the layer.

Both sides of the layer are decorated by the phenyl rings of 1,2-bdc in a herringbone pattern with the phenyl rings on one side of the layer roughly perpendicular ($87.1(1)^\circ$) to the phenyl rings on the other side (Figure 2). In structure **2**, the layers are stacked by simple AA translation, leading to a chiral and polar structure with the space group symmetry $C2$. There are weak $\text{CH}-\pi$ type interactions between neighboring layers. The shortest distance between a hydrogen atom of one layer and a phenyl carbon atom of a neighboring layer is 2.997(5) Å (Figure 2a, and b). In structure **1**, half of the layers are the same as those of structure **2** while the other half are their mirror-image layers. The former and the latter are alternately stacked in **1** so that neighboring layers are related by an inversion center. In contrast to the case of structure **2**,

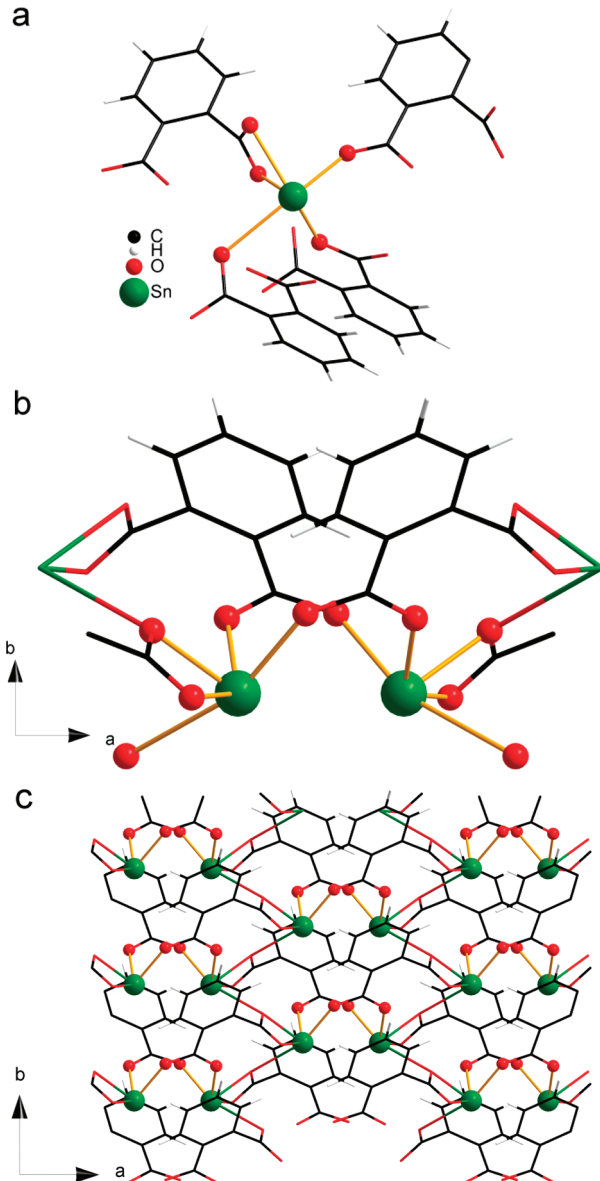


Figure 1. Coordination of the Sn atom (a), the “butterfly” unit (b), and an individual layer (c) in **2**. The color coding for the atoms is given in Figure 1a.

where the phenyl rings of neighboring layers are roughly perpendicular, in structure **1** the phenyl rings of neighboring layers are parallel to each other (the dihedral angle is 0 within the errors) (Figure 2c and d). The shortest distance between a hydrogen atom and a carbon atom of the phenyl group in the layer below is 3.10(1) Å, indicating weak $\text{CH}-\pi$ type interactions. Partial stacking disorder in the crystals of **1** is indicated by the diffuse nature of some reflections in the X-ray diffraction data and by the splitting of the electron density peaks around the Sn atom site in the calculated electron density maps. In the refinements the Sn position could be split into two sites that are 0.33 Å apart from each other. The Sn site with the majority occupancy (77%) is well-defined, but the other tin atom on the other Sn site with 23% occupancy has a very large thermal ellipsoid, probably due to the stacking disorder.

Crystal Structures of $\text{Sn}(1,3\text{-bdc})$ (3**).** The tetragonal structure of **3** contains one symmetry inequivalent tin atom that is asymmetrically coordinated by two oxygen atoms at 2.137(1) Å

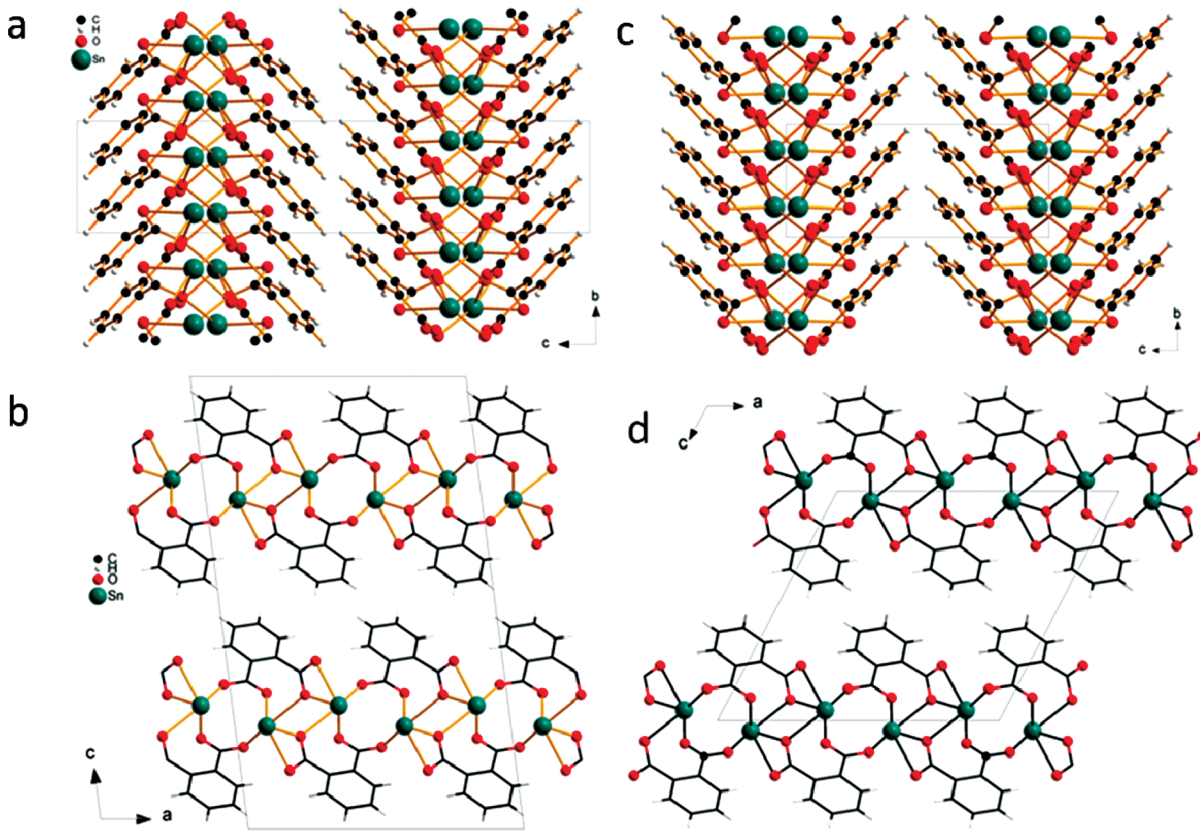


Figure 2. Views of the structures of **1** (a,b) and **2** (c,d), showing the different stacking of the layers and the orientations of the phenyl groups.

and two at 2.446(1) Å, as shown in Figure 3a. Each tin atom may also be considered to have four additional very weak bonds with bond lengths of 3.103(1) Å and 3.243(1) Å. The chains of tin atoms shown in Figure 3a are connected in pairs by the bdc ligands to form the tubular structure shown in Figure 3b. The longer weak bonds (3.243(1) Å) are found within the tubes and are shown as dotted blue lines.

In the three-dimensional structure, the tubes are arranged about the 4-fold axis as shown in Figure 3c. Each group of four chains are weakly bonded together by intertube Sn–O bonds (3.103(1) Å) as shown by the green dotted lines in the perspective view in Figure 3d.

Structure of $\text{Sn}_3\text{O}(1,4\text{-bdc})_2$ (4). The structure of **4** contains three inequivalent tin atoms. The three tin atoms are connected by one μ_3 oxygen atom (O9) with Sn–O bond lengths of 2.094(4), 2.085(5), and 2.079(3) Å. The Sn2 and Sn3 atoms are both four coordinated by the μ_3 oxygen atom, by two oxygen atoms from a chelating carboxylate group, and one from a bridging carboxylate. The Sn1 atom is three coordinated by the μ_3 oxygen atom and by two oxygen atoms from bridging carboxylate groups. The Sn_3O trimers are connected to form layers in the *ab* plane by bridging carboxylate anions that connect Sn1 to Sn2 (up) and Sn1 to Sn3 (down) as shown in Figure 4. The orientation of the phenyl groups relative to the layer is indicated by the “up–down” notation above. Similarly, the phenyl groups with chelating carboxylates are “up” for Sn3 and “down” for Sn2 (note the hole in the layer where the lone pairs are located).

The four nonequivalent bdc anions cross-link adjacent layers in the structure as shown in Figure 5. Strong π – π interactions occur between the phenyl rings located at $z = 0.5$. The angle between the neighboring phenyl ring planes is 0.5(1)° and the distance between the ring centers is as short as

3.4738(5) Å, but the phenyl rings are rotated 33.0(2)° relative to each other. Somewhat weaker π – π interactions occur between the phenyl rings located at $z = 0$, where the angle between the neighboring phenyl rings is 4.3(1)° and the distance between their centers is 3.7403(4) Å.

Discussion

The coordination environments of the tin atoms in all structures **1**–**4** are highly nonspherical, which is typical for divalent Sn^{II} cations. Wang and Liebau proposed an eccentricity parameter $|\Phi_i|$ to describe quantitatively such asymmetric coordination, and they observed positive correlations between $|\Phi_i|$ and calculated bond valence sums (BVS)_{*i*} for many lone-pair cations including Sn^{II} .²⁰ They ascribe the correlation to the stereoactivity of the electron lone pair of the central cations. As shown in Figure 6, the data calculated for the SnO_n polyhedra of the Sn^{II} benzenedicarboxylates show a similar correlation, although the BVS range is rather small and close to the oxidation number of Sn^{II} . It was noticed that compounds with high $|\Phi_i|$ values typically have high cation/anion ratios, which tend to induce the lone pair of Sn^{II} to act as a pseudoanion. In the case of benzenedicarboxylates, the oxygen atoms of the 1,2-bdc ligand are closer together than in 1,3-bdc and 1,4-bdc; therefore, the 1,2-bdc ligand tends to form local structures with a low cation/anion ratio. In Figure 6, $\text{Sn}(1,2\text{-bdc})$ shows a lower $|\Phi_i|$ value than other Sn^{II} benzene-carboxylates.

Layered structures formed by metal 1,2-benzenedicarboxylates are quite common. The layers are usually decorated by the phenyl rings on both sides. Typical examples include $\text{Cd}(1,2\text{-bdc})$ ²³ and $\text{KCo}(1,2\text{-bdc})(\text{OH})$.²⁴ However, polar layers with the phenyl rings arranged in a herringbone pattern

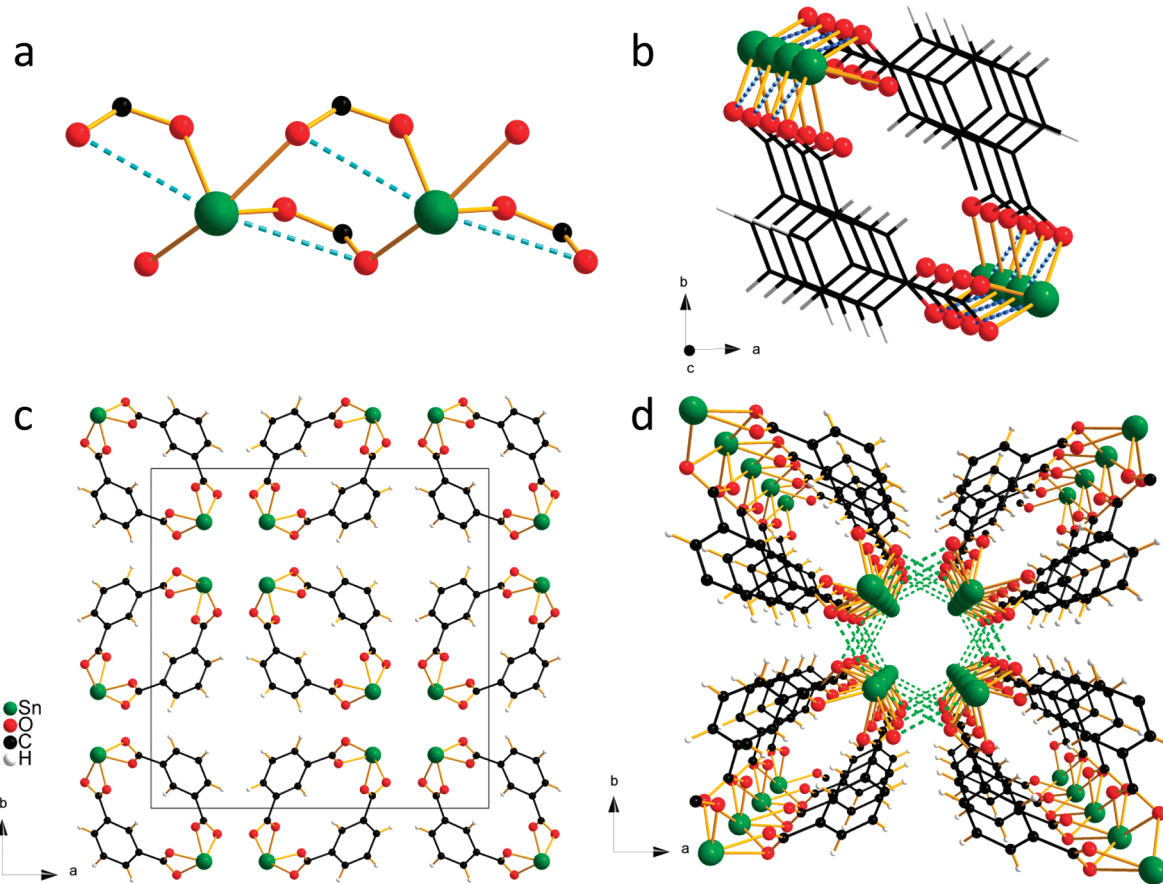


Figure 3. Structure of **3**, showing the tin oxide chain (a), the 1D tube (b), a parallel view (c), and a perspective view (d) along the tube axis. Blue and green dotted lines represent intra- and intertube weak Sn–O interactions, respectively.

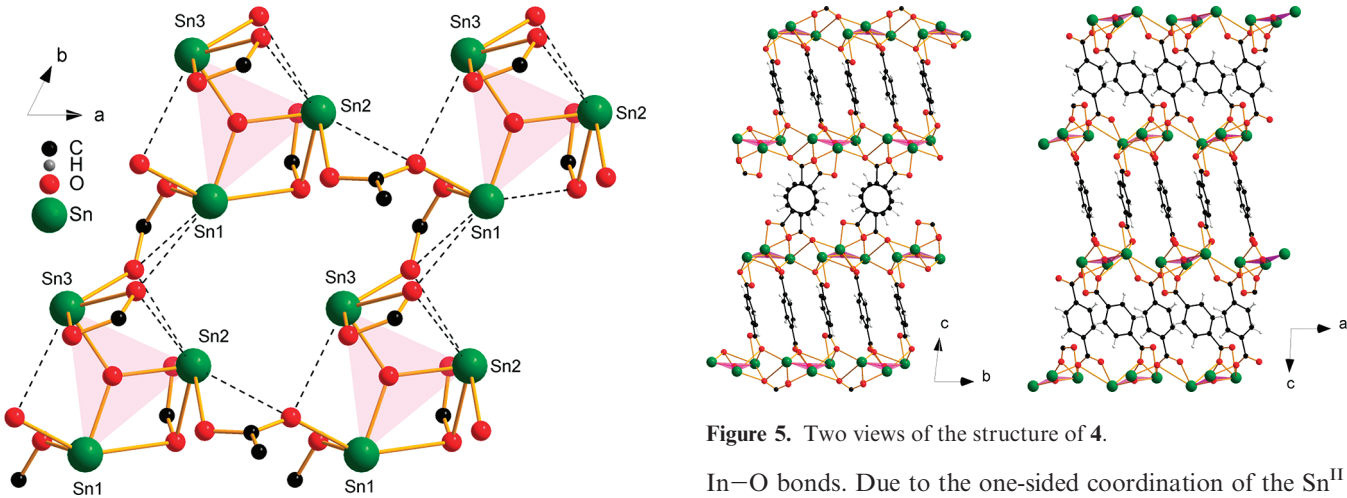


Figure 4. Sn_3O trimers in the structure of **4**, marked by red triangles.

as observed in structures **1** and **2** are rare. Such an arrangement may be related to the preferred orientation of the electron lone pair of the Sn^{II} cations in the layer. Since polarity is a prerequisite for some important physical properties such as pyroelectricity, it is encouraging that the individual polar layers can be stacked in a way that leads to the polar structure of **2**.

Recently, we reported open layers formed by indium cyclohexanedicarboxylates (chdc).²⁵ The open layers in the structure of $\text{In(OH)}(1,3\text{-chdc})$ are formed by fusing together tubular units similar to those of compound **3** through the

Figure 5. Two views of the structure of **4**.

In–O bonds. Due to the one-sided coordination of the Sn^{II} cations, the tubes in **3** are separated and the intertubular Sn–O bonds are very weak. Wider tubes are expected if the 1,3-bdc ligands in **3** could be replaced by larger bent ligands. 3D frameworks are observed both for compound **4** and for the $\text{A}_2\text{Sn}_2(1,4\text{-bdc})_3(\text{H}_2\text{O})_x$ phases,¹⁸ due to the bonding capability at both ends of the 1,4-bdc ligand. The Sn_3O triangle units of compound **4** are also found in other known divalent tin compounds. The configuration with the μ_3 oxygen atom at the center of the triangle is favored from a bond-valence point of view. The shortest Sn–O bond in a Sn^{II}O_n polyhedron usually has a bond valence of ca. $2/3$ v.u.; therefore, the valence sum of three such bonds matches the oxidation number of the oxygen ion. In the structure of $\text{Sn}_3\text{O}(\text{OH})_2(\text{SO}_4)$, the Sn_3O triangle is

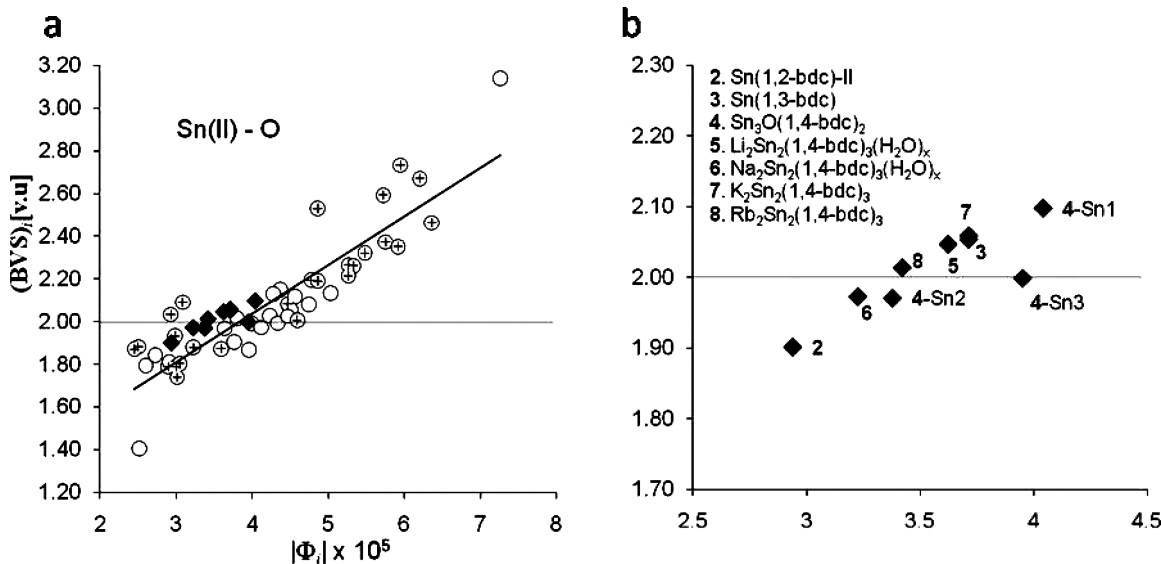


Figure 6. Correlation between the eccentricity parameter $|\Phi_i|$ and bond valence sums (BVS) calculated by using the Brese and O’Keeffe parameter.²¹ (a) The circles and the fitted line are from ref 20. Crosses are the data points rechecked recently by Brown with more stringent criteria.²² Black diamonds are data for the Sn^{II} benzenedicarboxylates. (b) Data for the Sn^{II} benzenedicarboxylates with labels. Data for $\text{A}_2\text{Sn}_2(\text{bdc})_3(\text{H}_2\text{O})_x$ are from ref 18. Compound 1 and $\text{Cs}_2\text{Sn}_2(\text{bdc})_3$ are not considered because of the structure disorder.

interconnected by the sulfate tetrahedra.²⁶ In $\text{Sn}_5\text{O}_2(\text{PO}_4)_2$ two Sn_3O triangles share a common Sn corner to form a Sn_5O_2 unit that is linked by the phosphate tetrahedra,²⁷ while in $\text{Sn}_2\text{O}(\text{C}_4\text{O}_4)(\text{H}_2\text{O})$ two Sn_3O triangles share a common edge to form a Sn_4O_2 unit that is linked by the squareate anions.²⁸ The Sn_5O_2 and Sn_4O_2 units have not been observed in the tin benzenedicarboxylate systems. Given the interesting variations in linking the OSn_3 triangle units, more divalent tin benzenedicarboxylate structures are anticipated.

Acknowledgment. We thank the R. A. Welch Foundation, NHARP—Chemistry 003652-0092-2007, and NSF DMR-0706072 for support of this work.

Supporting Information Available: Crystal data, thermogravimetric analysis data, powder X-ray diffraction data, and X-ray crystallographic information files (CIF) for compounds **1–4**. This information is available free of charge via the Internet at <http://pubs.acs.org/>.

References

- Yaghi, O. M.; O’Keeffe, M.; Ockwig, N. W.; Chae, H. K.; Eddaoudi, M.; Kim, J. *Nature (London, U. K.)* **2003**, *423*, 705–714.
- Ferey, G. *Chem. Soc. Rev.* **2008**, *37*, 191–214.
- Perry, J. J. t.; Perman, J. A.; Zaworotko, M. J. *Chem. Soc. Rev.* **2009**, *38*, 1400–17.
- Rao, C. N. R.; Cheetham, A. K.; Thirumurugan, A. *J. Phys.: Condens. Matter* **2008**, *20*, 083202/1–083202/21.
- Vougo-Zanda, M.; Huang, J.; Anokhina, E.; Wang, X.; Jacobson, A. J. *Inorg. Chem.* **2008**, *47*, 11535–11542.
- Go, Y.; Wang, X.; Anokhina, E. V.; Jacobson, A. J. *Inorg. Chem.* **2004**, *43*, 5360–5367.
- Go, Y. B.; Wang, X.; Anokhina, E. V.; Jacobson, A. J. *Inorg. Chem.* **2005**, *44*, 8265–8271.
- Harrison, P. G. *Chemistry of Tin*; Blackie & Son Ltd: Glasgow, 1989.
- Donaldson, J. D.; Grimes, S. M. *Rev. Silicon, Germanium, Tin Lead Compd.* **1984**, *8*, 1–132.
- Harrison, P. G.; Steel, A. T. *J. Organomet. Chem.* **1982**, *239*, 105–13.
- Davidovich, R. L.; Stavila, V.; Marinin, D. V.; Voit, E. I.; Whitmire, K. H. *Coord. Chem. Rev.* **2009**, *293*, 1316–1352.
- Harrison, P. G.; Thornton, E. W. *J. Chem. Soc., Dalton Trans.* **1978**, 1274–8.
- Donaldson, J. D.; Donoghue, M. T.; Smith, C. H. *Acta Crystallogr., Sect. B* **1976**, *B32*, 2098–101.
- Natarajan, S.; Vaidhyanan, R.; Rao, C. N. R.; Ayyappan, S.; Cheetham, A. K. *Chem. Mater.* **1999**, *11*, 1633–1639.
- Salami, T. O.; Marouchkin, K.; Zavilij, P. Y.; Oliver, S. R. *J. Chem. Mater.* **2002**, *14*, 4851–4857.
- Ramaswamy, P.; Datta, A.; Natarajan, S. *Eur. J. Inorg. Chem.* **2008**, 1376–1385.
- Sun, J.-Y.; Zhou, Y.-M.; Chen, Z.-X.; Tu, B.; Weng, L.-H.; Zhao, D.-Y. *Gaodeng Xuexiao Huaxue Xuebao* **2003**, *24*, 1555–1557.
- Wang, X.; Liu, L.; Makarenko, T.; Jacobson, A. J. *J. Cryst. Growth Des.* **2010**, *10*, 1960–1965.
- APEX2 User Manual*, Version 1.27; Bruker AXS Inc.: Madison, WI, 2005.
- Wang, X.; Liebau, F. *Acta Crystallogr., Sect. B: Struct. Sci.* **2007**, *B63*, 216–228.
- Brese, N. E.; O’Keeffe, M. *Acta Crystallogr., Sect. B: Struct. Sci.* **1991**, *B47*, 192–7.
- Brown, I. D. *Acta Crystallogr., Sect. B: Struct. Sci.* **2009**, *B65*, 684–693.
- Tang, Y.-Z.; Qian, S.-S.; Wang, X.-S.; Zhao, H.; Huang, X.-F.; Li, Y.-H.; Jiao, X.-C.; Xiong, R.-G. Z. *Anorg. Allg. Chem.* **2004**, *630*, 1623–1626.
- Cheng, X.-N.; Xue, W.; Zhang, W.-X.; Chen, X.-M. *Chem. Mater.* **2008**, *20*, 5345–5350.
- Kim, I.-H.; Wang, X.; Jacobson, A. J. *Solid State Sci.* **2010**, *12*, 76–82.
- Grimvall, S. *Acta Chem. Scand., Ser. A* **1975**, *A29*, 590–8.
- Yuan, X.; Li, Y.-Z.; Xu, Y.; You, X.; Linhardt, R. J. *Eur. J. Inorg. Chem.* **2007**, 858–864.
- Millet, P.; Sabadie, L.; Galy, J.; Trombe, J. C. *J. Solid State Chem.* **2003**, *173*, 49–53.